ISSN 0023-1584, Kinetics and Catalysis, 2010, Vol. 51, No. 1, pp. 88–97. © Pleiades Publishing, Ltd., 2010.
Original Russian Text © V.Yu. Gavrilov, O.P. Krivoruchko, T.V. Larina, I.Yu. Molina, R.A. Shutilov, 2010, published in Kinetika i Kataliz, 2010, Vol. 51, No. 1, pp. 95–105.

Distribution of Copper- and Nickel-Containing Modifier Components in the Pore Space of HZSM-5 Zeolite

V. Yu. Gavrilov, O. P. Krivoruchko, T. V. Larina, I. Yu. Molina, and R. A. Shutilov

Boreskov Institute of Catalysis, Siberian Branch, Russian Academy of Sciences, Novosibirsk, 630090 Russia

e-mail: gavrilov@catalysis.ru

Received August 6, 2008

Abstract—The distribution of copper- and nickel-containing components in the pore space of HZSM-5 zeolite was quantitatively studied. It was found that the detailed distribution of a modifier in the micropore and mesopore volumes of the zeolite depends on both the chemical nature of the modifier and the conditions of supporting and the regime of M^{2+} polycondensation in the pore space of the zeolite. The experimental data on the low-temperature adsorption of nitrogen on Cu(*n*)ZSM-5 catalysts can be interpreted as the result of the partial filling of the zeolite micropore space (10 vol %) and the finest mesopores with $D < 3$ nm with the modifier. In the case of Ni(*n*)ZSM-5 catalysts, the penetration of the modifier into zeolite channels (micropores) in detectable amounts was not found, and it was arranged in mesopores on the surface of zeolite crystallites. The reason for differences between modifier distributions in the pore structure of the zeolite was explained from the standpoint of different structures of copper and nickel polyhydroxo complexes in impregnating solutions after polycondensation. It was found that, in the Cu(*n*)ZSM-5 and Ni(*n*)ZSM-5 catalysts, the modifier component contained copper and nickel only in a doubly charged state and mainly octahedral oxygen environments. In this case, three-dimensional nanoparticles or coarsely dispersed particles of CuO were not detected in the pore space of the support, whereas the presence of a small amount of sufficiently large NiO crystals with a coherent-scattering region of 80–100 nm was detected in Ni(*n*)ZSM-5, and these crystals occurred on the surface of zeolite crystals. It was found that the apparent density of a copper- or nickel-containing component arranged in the pore space of the zeolite was lower than the density of the bulk CuO and NiO phases by a factor of ~3 and 4, respectively, because of the size effect.

DOI: 10.1134/S0023158410010155

INTRODUCTION

High-silica HZSM-5 zeolites are widely used in the large-scale processes of oil refining and petroleum chemistry. Catalysts based on HZSM-5 play an important role in the neutralization of harmful exhaust emissions from motor transport and industry. The modification of zeolites with doubly charged cations, in particular, Cu^{2+} and Ni^{2+}, makes it possible to purposefully control their functional properties, namely, acid–base, redox, and electronic properties and the activity, selectivity, coking ability, regenerability, and thermal stability of catalysts, which depend on the above properties.

Of the two systems tested in this study, CuZSM-5 zeolites are more commonly used as catalysts. They are active in the reactions of NO [1–6] and N_2O [6, 7] decomposition to N_2 and O_2, in the selective reduction of NO_x to N_2 with various hydrocarbons (other than methane) [8–11], in the aromatization reactions of ethylene [12] and *n*-butane [13], in the alkylation of benzene with propane [14], and in the hydroxylation of benzene to phenol in an atmosphere of O_2 or O_2/H_2 [15].

Unlike CuZSM-5, the NiZSM-5 catalysts can conduct the reactions of selective NO_x reduction with methane [16, 17] and CH_4 reforming with carbon dioxide [18, 19]. They are also active in the aromatization of propane [20], *n*-butane [13], pentane [21], and hexane [22] and in the alkylation of benzene with propane [14]; they exhibit unusual acid properties and adsorption capacity for H_2 [23].

Usually, these catalysts are prepared by the modification of high-silica HZSM-5 zeolite with M^{2+} cations using ion exchange in accordance with a wet or dry technology. The optimum concentration of a modifier component is found from the experimental dependence of activity (selectivity) on the concentration of M^{2+}. In this case, as a rule, the coordination environment and oxidation state of the metal, as well as the distribution of the modifier component in the zeolite pore space, remain unknown. At the same time, the nonlinear dependence of the activity of CuZSM-5, for example, in NO decomposition reactions, on the total Cu^{2+} concentration was reported [3]. Evidently, this suggests that the modifier component consists of several $Cu_x–O_y–H_z$ species having different dependences of activity on the Cu^{2+} content of the catalyst.

According to published data, ion exchange is performed in the suspensions of HZSM-5 zeolites in

aqueous solutions of Cu^{2+} or Ni^{2+} salts (primarily as M^{2+} acetates or nitrates) with concentrations from 0.001 to 1.0 mol/l in different studies. The M^{2+} modifier component of catalysts is tentatively subdivided into the following two portions: ion-exchange and superexchange. The first portion contains M^{2+} cations at charge-exchange sites of three types depending on the Si/Al ratio in the zeolite and the conditions of impregnation [23–25]. The second portion is hypothetically described as the polynuclear hydroxo complexes of M^{2+} localized at the ion-exchange sites of the HZSM-5 zeolite framework in an unintelligible manner.

In a number of studies [1–5], it was found that superexchange Cu^{2+} ions make the main contribution to the activity of CuZSM-5 catalysts, for example, in the reaction of NO decomposition. The fraction of these ions in the catalysts increases as the salt concentration in impregnation solutions is increased; however, it increases most dramatically upon the forced hydrolysis of the aqua cations of Cu^{2+} by adding a base to solutions or a suspension [3, 26, 27]. A disadvantage of these procedures is the formation of not only mononuclear complexes but also of a set of polynuclear hydroxo complexes in salt solutions. In principle, this hinders the subsequent penetration of these species into the micropore part and fine mesopores of the parent zeolite.

We developed a procedure [28, 29], according to which the modifier component is initially introduced into zeolite by incipient wetness impregnation with aqueous M^{2+} solutions and then the hydrolytic polycondensation of the cations that occurred in zeolite pores was performed by the treatment of the solutions with dilute NH_3 solutions at pH ~ 9. However, in this case, as well as in published works, the coordination environment and oxidation state of cations, as well as the distribution of a modifier component in the zeolite pore space, remained undetermined; this did not allow us to improve the performance characteristics of catalysts on a scientific basis.

The aim of this work was to study the distribution and electronic states of copper- and nickel-containing modifiers in the pore space of the ZSM-5 catalyst.

EXPERIMENTAL

The catalysts tested in this study were synthesized by postsynthetic modification. The series of Cu(*n*)ZSM-5 and Ni(*n*)ZSM-5 samples, where *n* is the Cu content from 0.5 to 5.0 wt % or Ni content from 1.0 to 5.0 wt % on a zeolite sample basis, were studied. Commercial HZSM-5 zeolite with the ratio Si/Al = 17 and Fe^{3+} and Na^+ impurity concentrations of 0.09 and 0.05 wt %, respectively, with no binder was used for the synthesis of the catalysts. The degree of crystallinity of the used zeolite was no lower than 95%, as determined by a quantitative comparison of X-ray data with those for a reference sample of HZSM-5. The zeolite was calcined at 300°C to constant weight before introducing Cu^{2+} or Ni^{2+} ions. The cations were introduced into the zeolite by incipient wetness impregnation with the aqueous solutions of corresponding chlorides (of analytical grade) at pH 2. The use of acidified water allowed us to prevent the hydrolysis of aqua M^{2+} cations at the stage of the preparation of salt solutions. Then, the zeolite powder containing an impregnation solution of M^{2+} salts was treated with a dilute solution of NH_3 at pH 9 and room temperature; the solid phase was filtered off, washed with distilled water, and kept in air to a dry state. At the final stage of the synthesis, the samples were dried and calcined in air at 110 and 450°C, respectively, for 6 h at either of the temperatures. Here, we report the results of a study of the samples calcined at a final temperature of 450°C. Note that the concentrations of Cu^{2+} and Ni^{2+} in the impregnation solutions were varied from ~0.1 to 1.0 mol/l.

The distribution of a Cu or Ni modifier component in the zeolite catalysts was studied in accordance with an adsorption method by measuring and treating the isotherms of the low-temperature (77 K) adsorption of nitrogen vapor on an automated DigiSorb 2600 instrument from Micromeritics. The catalyst samples were preliminarily trained under vacuum conditions at 10^{-3} Torr and 250°C for 5 h to remove water vapor from the pore space of the zeolite.

The experimental isotherms of nitrogen adsorption were processed using a comparative method [30] in order to calculate the micropore volumes (V_μ, cm^3/g) and mesopore surface areas (S_α, m^2/g). The mesopore size distribution and the cumulative mesopore volume (V_{cum}, cm^3/g) were calculated using the Barett–Joyner–Halenda (BJH) method [31].

The electronic diffuse reflectance spectra were measured on a UV-2501 PC spectrophotometer from Shimadzu with an ISR-240 A diffuse reflectance attachment. The samples as powder were placed in a quartz cell with an optical path length of 2 mm. The spectra were measured with reference to a $BaSO_4$ reflection standard over the range of 11000–53000 cm^{-1}. The resulting electronic diffuse reflectance spectra were plotted in the Kubelka–Munk function $F(R)$–wavenumber coordinates.

The X-ray diffraction patterns of HZSM-5 and Me^{2+}(*n*)ZSM-5 samples were measured on an ARL X'TRA diffractometer by point-by-point scanning at a 2θ step of 0.05° and an accumulation time of 3 s in the region of 2θ = 5°–60°.

RESULTS AND DISCUSSION

Figure 1 shows the adsorption isotherms of nitrogen vapor on Cu(*n*)ZSM-5 catalysts. It can be seen that a developed mesopore volume occurred in the samples along with the micropore structure of the zeolite; this volume was responsible for the capillary con-

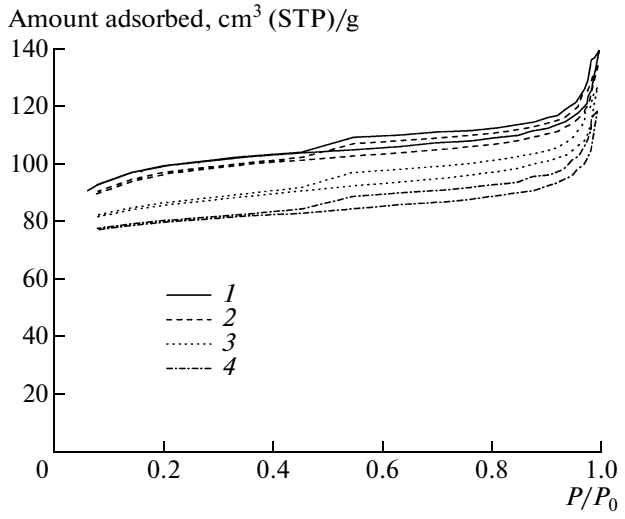

Fig. 1. Isotherms of nitrogen adsorption (77 K) on Cu(*n*)ZSM-5 catalysts: *n* = (*1*) 0.5, (*2*) 1, (*3*) 2, and (*4*) 3 wt %.

densation of the sorbate and the occurrence of a corresponding hysteresis in the isotherm.

Table 1 summarizes the main texture parameters calculated from the experimental adsorption isotherms. In this case, for a correct comparison, the parameters (*P*) were referred to 1 g of zeolite in the catalyst using the obvious relationship $P(1 + X)$, where X is $g_{Cu}/g_{zeolite}$.

As follows from Table 1, the modification of the zeolite with Cu^{2+} compounds resulted in changes in both the micropore texture component (a decrease in the micropore volume V_μ—the space within channels in zeolite crystallites) and the mesopore structure, likely, the space between zeolite crystallites.

A decrease in the micropore volumes of catalysts, as compared with that of the starting zeolite ΔV_μ suggests the partial arrangement of the modifier in zeolite channels. Simultaneously, the total micropore and mesopore volume V_s decreased by ΔV_s and the specific surface area of mesopores S_α decreased. Obviously, this was a consequence of the modifier distribution on the mesopore volume, that is, on the surface of zeolite crystallites.

The parameter $\gamma = \Delta V_\mu/\Delta V_s$ is a measure of the volume fraction of the copper-containing modifier arranged in micropores with reference to the total amount of this modifier. The absence of the values of γ from samples with minimum modifier contents was related to an insignificant change in the total pore volume, which was comparable with the real experimental error.

The data given in Table 1 indicate that, as would be expected, a decrease in the volume fraction of a modifier (γ) with increasing its weight in the catalysts (*n*) is a consequence of a constant degree of filling of zeolite channels in the course of modification. Indeed, we estimated that, on a priori assumption that the modifier density (ρ_m) in zeolite channels is constant, the modifier volume in micropores $\beta = n\gamma$ was approximately constant, 0.01 (cm^3 modifier in micropores)/g for samples with $n > 1\%$. Comparing this value with the micropore volume of 0.103 cm^3/g ($\lambda = \beta/V_\mu$) in HZSM-5, we obtained that the limiting degree of filling of zeolite channels with the modifier at any modifier amount was constant: $\lambda = U\rho_m = 0.1\rho_m$ (g modifier)/(cm^3 micropores), where U is the volume fraction of micropores occupied by the modifier (~10 vol %).

At the same time, note that the above estimation of zeolite channel filling with the modifier can, in principle, depend on the ratio between the sizes of the probe molecule (in this case, nitrogen with $\sigma_k = 0.364$ nm) and the zeolite channel ($d \sim 0.55$ nm) and the size of the modifier fragment. The possibility of partially blocking zeolite channels to nitrogen molecules by modifier clusters arranged on the crystallite surface cannot be finally excluded. A change in the size of the probe molecule, for example, the use of molecular hydrogen ($\sigma_k = 0.289$ nm) will allow one to subsequently study in detail the structure and arrangement of the modifier in the micropore channels of the zeolite.

Let us consider the distribution of the modifier in the mesopore volume of the support. Figure 2 compares the isotherms of nitrogen desorption on the parent HZSM-5 zeolite and the catalysts. This treatment was performed analogously to [29], where we previously considered the distribution of a cobalt-containing modifier in the pore structure of a zeolite catalyst prepared by an analogous synthesis method.

Table 1. Pore structure parameters of Cu(*n*)ZSM-5 catalysts

Sample	V_μ, cm^3/g	S_α, m^2/g	V_s, cm^3/g	V_{cum}, cm^3/g	ΔV_μ, cm^3/g	ΔV_s, cm^3/g	γ
ZSM-5	0.103	129	0.219	0.092	–	–	–
$n = 0.5\%$	0.102	121	0.221	0.096	0.001	–	–
$n = 1\%$	0.101	123	0.220	0.097	0.002	–	–
$n = 2\%$	0.098	117	0.209	0.088	0.005	0.010	0.5
$n = 3\%$	0.098	101	0.207	0.094	0.005	0.012	0.4
$n = 5\%$	0.096	54	0.182	0.082	0.007	0.037	0.2

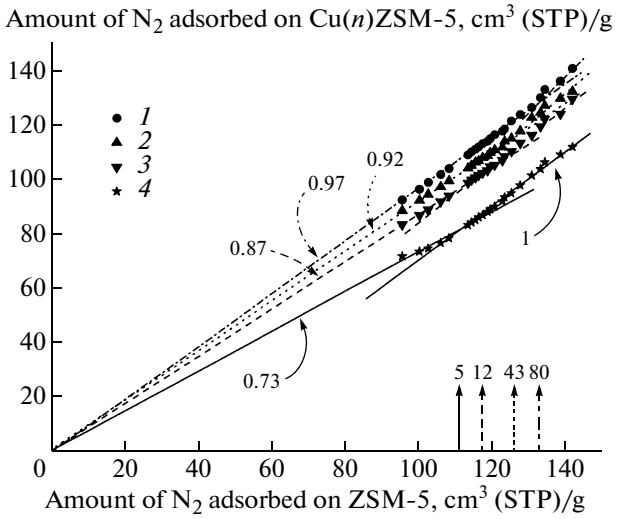

Fig. 2. Comparison between the isotherms of N_2 desorption on the parent HZSM-5 zeolite and modified Cu(*n*)ZSM-5 samples: *n* = (*1*) 1, (*2*) 2, (*3*) 3, and (*4*) 5 wt %. The slopes of comparative plots are specified in the figure.

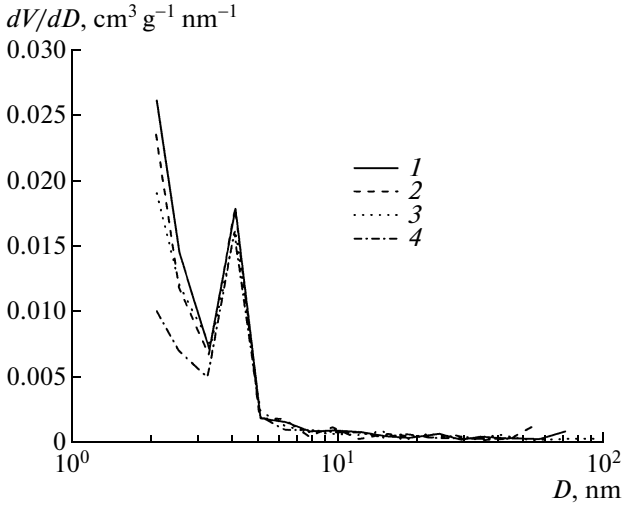

Fig. 3. Differential mesopore size distribution curves for (*1*) the parent HZSM-5 zeolite and (*2–4*) Cu(*n*)ZSM-5 catalysts: *n* = (*2*) 2, (*3*) 3, and (*4*) 5 wt %.

In Fig. 2, it can be seen that the slope of the initial portions of the isotherms decreased (from 0.97 to 0.73) with increasing modifier concentration. This is indicative of the predominant filling of the finest mesopores with the modifier to cause a considerable decrease in the specific surface area of mesopores S_α (Table 1). At the same time, the slopes of certain regions in the comparative plots remained almost unchanged with respect to the parent support; this fact suggests that corresponding structure regions remained unaffected; that is, the modifier was absent in these pores (the boundaries of the regions are marked with arrows in Fig. 2). The apparent paradoxicality of the result that the boundary of modifier occurrence shifts to the region of fine mesopores as the modifier amount is increased can be explained by the redistribution of the hydroxo complexes of Cu^{2+} with different nuclearities such that the proportion of polynuclear species increases as the total copper concentration in the impregnation solution is increased (in the course of the synthesis of catalyst samples with different compositions, this concentration was changed by one order of magnitude). This phenomenon will be considered in detail below.

Figure 3 shows differential mesopore-size distribution curves obtained by the BJH method for the Cu/ZSM-5 catalysts. It can be seen that the volumes of the finest mesopores with $D < 3.2$ nm decreased to the greatest extent; in general, this is consistent with the above results.

Based on the experimental data, we can estimate the apparent density of the modifier in the pore space of the zeolite. It will be demonstrated below that the modifiers contained copper and nickel only in a doubly charged state. The apparent density is estimated from the relation $\rho_{app} = m_{CuO}/\Delta V_s$ (the modifier weight should be increased based on the assumed CuO modifier composition using the ratio (63 + 16)/63 = 1.25). The calculations demonstrated that $\rho_{app} \approx 2.1$ g/cm^3. Note that the density of the CuO bulk phase is 6.4 g/cm^3.

Figure 4 shows the isotherms of nitrogen adsorption on Ni(*n*)ZSM-5 catalysts after treatment at 450°C. They also indicate that the test samples were characterized by developed micro- and mesoporosity.

The structure parameters given in Table 2 (as previously, they are referred to 1 g of zeolite in the catalyst) suggest that the micropore volume in the zeolite

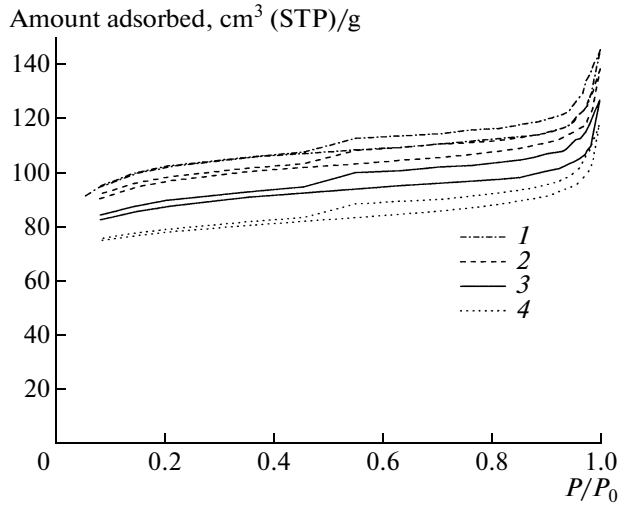

Fig. 4. Isotherms of nitrogen adsorption (77 K) on (*1*) the parent HZSM-5 zeolite and (*2–4*) Ni(*n*)ZSM-5 catalysts: *n* = (*2*) 1, (*3*) 3, and (*4*) 5 wt %.

Table 2. Pore structure parameters of Ni(*n*)ZSM-5 catalysts

Sample	V_μ, cm^3/g	S_α, m^2/g	V_s, cm^3/g	ΔV_s, cm^3/g	ρ_{app}, g/cm^3
ZSM-5	0.101	133	0.226	–	–
$n = 1\%$ Ni	0.101	118	0.217	0.009	1.4
$n = 3\%$ Ni	0.101	95	0.203	0.023	1.6
$n = 5\%$ Ni	0.102	60	0.191	0.035	1.8

remained unchanged. This can serve as evidence for the absence of a nickel-containing modifier in zeolite micropores (channels). Correspondingly, the modifier was arranged only in the mesopore fraction of the texture of the surface of zeolite crystallites. As in the case of a copper-containing modifier, the distribution of the nickel-containing modifier in mesopores was accompanied by a decrease in the total micro- and mesopore volume V_s and a decrease in the specific surface area of mesopores S_α.

Figure 5 compares the isotherms of nitrogen desorption on the parent HZSM-5 zeolite and nickel-containing catalysts. Unlike data shown in Fig. 2, in this case, the isotherms did not exhibit pronounced inflections and consisted of a linear portion. The value of the slope decreased linearly with an increasing modifier concentration *n*.

The linearity of the comparative plots of nitrogen desorption isotherms suggests the mainly uniform distribution of the modifier in the mesopore volume of the zeolite, whereas a linear correlation between the tangent value of the isotherms slope of the plots and the weight concentration of the modifier suggests that the apparent density of the modifier remained almost unchanged regardless of its concentration.

The distribution of the nickel-containing modifier on the external surface of HZSM-5 zeolite crystallites can result in the partial blocking (narrowing) of channel throats on the crystallite surface. This will cause an insignificant hysteresis of adsorption and desorption branches in the region of low relative pressures outside of the capillary-condensation hysteresis. Indeed, in Fig. 4, it can be seen that the isotherms on catalysts exhibited this hysteresis unlike isotherms on the parent zeolite.

Table 2 summarizes the values of the apparent density ρ_{app} of the nickel-containing modifier estimated in accordance with the above procedure. It can be seen that these values are close to each other; however, they are much different from the density of bulk NiO ($6.8\ g/cm^3$). Note that the values of ρ_{app} for this system characterize the properties of the nickel-containing modifier arranged only in the mesopore volume.

Figure 6 shows differential mesopore-size distribution curves for the Ni(*n*)ZSM-5 catalysts. It can be seen that, in this case, a change in the character of the distribution of fine mesopores was much smaller than that in the case of the distribution of the copper-containing modifier (Fig. 3) at comparable amounts of the introduced modifiers.

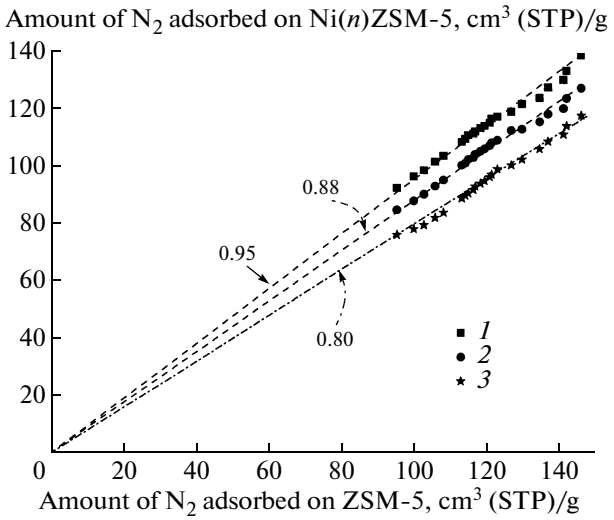

Fig. 5. Comparison between the isotherms of N_2 desorption on the parent HZSM-5 zeolite and modified Ni(*n*)ZSM-5 samples: $n = (1)$ 1, (*2*) 3, and (*3*) 5 wt %. The slopes of comparative plots are specified in the figure.

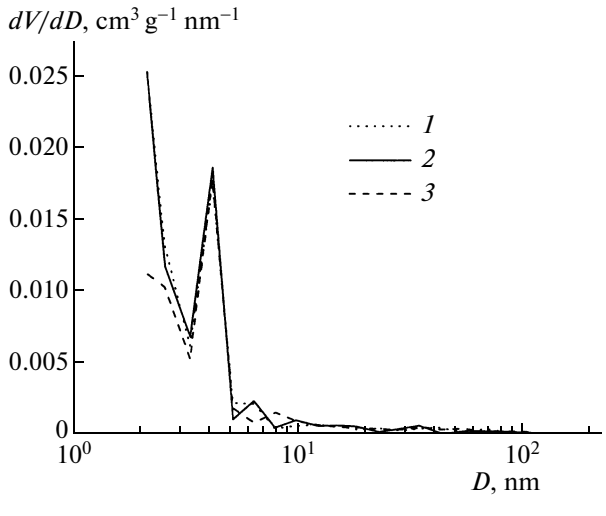

Fig. 6. Differential mesopore size distribution curves for Ni(*n*)ZSM-5 catalysts: $n = (1)$ 1, (*2*) 3, and (*3*) 5 wt %.

Table 3. Parameters of the distribution of modifier components in the pore space of ZSM-5 zeolite

Component	n, wt %	U, $(cm^3_{modifier})/(cm^3_{micropore})$	Region I of the isotherm (tangent of slope)	Region II of the isotherm (tangent of slope)
Ni^{2+}	1	0	0.95	
	3		0.88	
	5		0.80	
Cu^{2+}	2	0.1	0.92 (43)	1
	3		0.87 (12)	1
	5		0.73 (5)	1
Co^{2+} [24]	2	0.16	0.90	0.90
	3	0.17	0.76	0.89
	5	0.27	0.61	0.81

* Pore diameters (nm) corresponding to the boundary between regions I and II of comparative plots are given in parentheses.

Thus, we can state that the distribution of the modifier component in the test nickel-containing catalysts occurred uniformly in the pore space of mesopores with localization on the surface of zeolite crystallites. In this case, the penetration of the nickel-containing component into micropore channels was not observed.

For comparison, Table 3 summarizes experimental data on the occurrence of copper- and nickel-containing modifiers and published data [29] on the distribution of a cobalt-containing modifier in the pore space of HZSM-5 zeolite.

In Table 3, it can be seen that the distribution of a modifier depends on its chemical nature. Thus, the nickel-containing modifier was fully arranged in mesopores; it is believed that its arrangement is independent of mesopore sizes.

The copper-containing modifier occupied approximately 10% of the zeolite channel volume, whereas the remaining portion was arranged in mesopores on the surface of zeolite crystallites. In this case, as the amount of the introduced modifier was increased, it was mainly arranged in finer mesopores. Table 3 shows (in parentheses) pore diameters (in nm) corresponding to the boundary between regions I and II in the comparative plots. In large mesopores (region II of the comparative plots), the arrangement of the copper-containing modifier did not occur.

To draw a general conclusion, we can state that, in the modification of zeolite with a cobalt-containing component, the occupation of micropores (U) increased as the introduced amount (n) was increased. Simultaneously, the modifier was also arranged in the mesopore volume. In this case, two regions of mesopores with different pore sizes can be recognized; the degrees of filling of these regions with the modifier were different.

Let us consider the diffuse reflectance electronic spectroscopy data for the parent HZSM-5 zeolite and the modified Cu(n)ZSM-5 and Ni(n)ZSM-5 samples.

Figure 7 shows the diffuse reflectance electronic spectra of unmodified HZSM-5 and Cu(n)ZSM-5 samples obtained by modifying the HZSM-5 zeolite with Cu^{2+} cations with concentrations from 0.5 to 5.0 wt %. The parent zeolite (Figs. 7 and 8, curves *1*) was characterized by the appearance of a characteristic absorption edge in the UV region at 34500 cm^{-1} due to the occurrence of a bandgap typical of dielectric oxide structures in zeolite [32]. The absence of absorption bands from the visible region of the diffuse reflectance electronic spectra of parent HZSM-5 due to the absorption of the zeolite as a whole allowed us to unambiguously interpret the absorption bands that characterize the electronic state of M^{2+} in the modifier component of M^{2+}(n)ZSM-5 samples.

The Cu(0.5)ZSM-5 sample (Fig. 7, curve *2*) exhibited an absorption band at 12000 cm^{-1} in the visible region of the electronic diffuse reflectance spectrum and absorption bands at 27700 and 48500 cm^{-1}

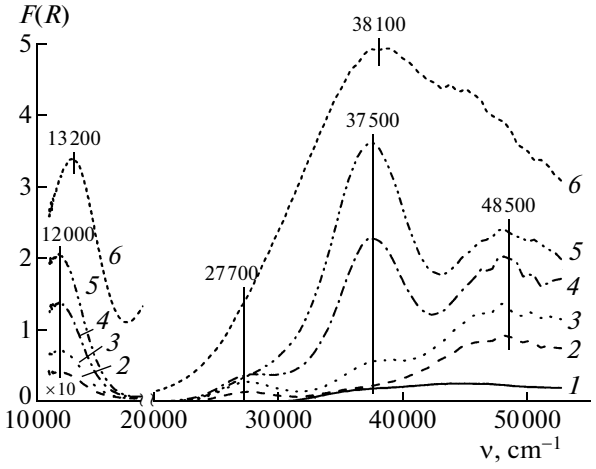

Fig. 7. Electronic diffuse reflectance spectra of (*1*) the parent HZSM-5 zeolite and (*2–6*) modified Cu(n)ZSM-5 samples: n = (*2*) 0.5, (*3*) 1, (*4*) 2, (*5*) 3, and (*6*) 5 wt %.

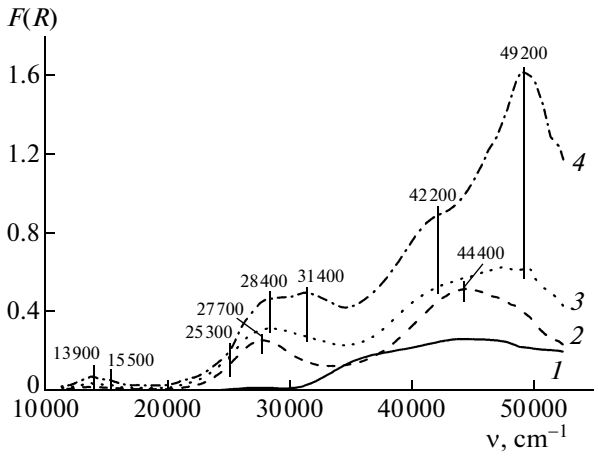

Fig. 8. Electronic diffuse reflectance spectra of (*1*) the parent HZSM-5 zeolite and modified Ni(*n*)ZSM-5 samples: *n* = (*2*) 1, (*3*) 3, and (*4*) 5 wt %.

(the latter was more intense) in the UV region of the spectrum. The low-intensity absorption band at 12000 cm^{-1} was due to the *d*–*d* transition of Cu^{2+} cations in an octahedral oxygen coordination (Cu^{2+}_{Oh}) stabilized at the ion-exchange positions of HZSM-5 zeolite. It is most likely that the intense absorption band at 48500 cm^{-1} was a ligand–metal charge-transfer (CT) band of Cu^{2+}_{Oh} cations, which was observed previously in zeolite Y [33]. The absorption band at 27700 cm^{-1} can be attributed to compounds like $Al_x(OH)_y$, although this hypothesis should be additionally tested. As the concentration of Cu^{2+} cations in Cu(*n*)ZSM-5 zeolite was increased from 1.0 to 3.0 wt % (Fig. 7, curves *3*–*5*), a ligand–metal CT band at 37500 cm^{-1} appeared in the electronic diffuse reflectance spectrum and its intensity dramatically increased with the copper content of the sample. It is most likely that this absorption band was due to oxygen-containing one- and/or two-dimensional Cu^{2+}_{Oh} nanoclusters. As the concentration of Cu^{2+} cations in Cu(*n*)ZSM-5 zeolite was increased to 5.0 wt % (Fig. 7, curve *6*), a shift in the absorption band due to the *d*–*d* transition in Cu^{2+} cations from 12000 to 13200 cm^{-1} and a shift in the ligand–metal CT band from 37500 to 38100 cm^{-1} were observed in the electronic diffuse reflectance spectrum. This suggests a tetragonal distortion in the oxygen tetrahedron around Cu^{2+} cations, which were most likely stabilized in the mesopores of HZSM-5 zeolite as two-dimensional clusters.

Thus, it follows from the electronic diffuse reflectance spectroscopic data that a portion of Cu^{2+}_{Oh} cations in the Cu(*n*)ZSM-5 samples was stabilized at the ion-exchange positions of HZSM-5 zeolite channels. As the concentration of Cu^{2+} cations in the Cu(*n*)ZSM-5 zeolite was increased from 1.0 to 3.0 and 5.0 wt %, the Cu^{2+} cations were also stabilized as oxygen-containing clusters in the mesopores of HZSM-5 zeolite.

Figure 8 shows the electronic diffuse reflectance spectroscopic data for Ni(*n*)ZSM-5 samples obtained by modification of HZSM-5 with 1.0, 3.0, and 5.0 wt % Ni^{2+} cations and for the initial zeolite HZSM-5, as in the case of the Cu(*n*)ZSM-5 samples presented in Fig. 7.

The Ni(1.0)ZSM-5 sample (Fig. 8, curve *2*) exhibited absorption bands at 13900 and 15500 cm^{-1} in the visible region of the electronic diffuse reflectance spectrum and more intense absorption bands at 27700 and 44400 cm^{-1} in the UV region of the spectrum. The low-intensity absorption bands at 13900 and 15500 cm^{-1} were due to the *d*–*d* transitions of Ni^{2+} cations in an octahedral oxygen coordination (Ni^{2+}_{Oh}) stabilized at the ion-exchange positions of HZSM-5 zeolite. It is most likely that the intense absorption bands at 27 700 and 44 400 cm^{-1} in the UV region of the electronic diffuse reflectance spectrum were due to the ligand–metal CT band of Ni^{2+}_{Oh} cations in the two-dimensional oxygen clusters $(-M^{2+}-O^{2-})_n$. An increase in the Ni^{2+} content of HZSM-5 to 3.0 wt % resulted in dramatic changes in the electronic diffuse reflectance spectrum in the UV region. The Ni(3.0)ZSM-5 zeolite (curve *3*) exhibited absorption bands with maximums at 28400 and 49200 cm^{-1} and shoulders at 25300, 31400, and 42200 cm^{-1}, which appeared as absorption bands at the same transition energies as the concentration of Ni^{2+} cations was increased to 5.0 wt % (Fig. 8, curve *4*). According to published data [34], absorption bands at 13900 and 15500 cm^{-1} and a shoulder at 25300 cm^{-1} were due to the *d*–*d* transitions of Ni^{2+}_{Oh} cations, which were likely stabilized at the ion-exchange positions of HZSM-5 zeolite channels. Becerra and Castro-Luna [35] studied the nature of the absorption spectra of bulk NiO and supported onto a carrier as a catalyst precursor. From a comparison between absorption spectra in [35], it follows that the bulk NiO oxide has absorption band intensities greater than those of supported NiO. This dependence of the intensity of absorption bands corresponds to a small amount of NiO in the supported sample (per unit sample weight), as compared with the bulk NiO oxide. According to Becerra and Castro-Luna [35], the intense absorption bands in the UV region at 31400 and 49200 cm^{-1} were due to the ligand–metal CT bands of Ni^{2+}_{Oh} cations in NiO oxide, which was most likely stabilized on the external surface of the powder particles of HZSM-5 zeolite in our case. Note that, in the electronic diffuse reflectance spectrum of the Ni(5.0)ZSM-5 zeolite (curve *4*), the absorption bands at 28400 and 42200 cm^{-1} belong to the ligand–metal CT absorption band of Ni^{2+}_{Oh} cations present in the two-dimensional oxygen clusters

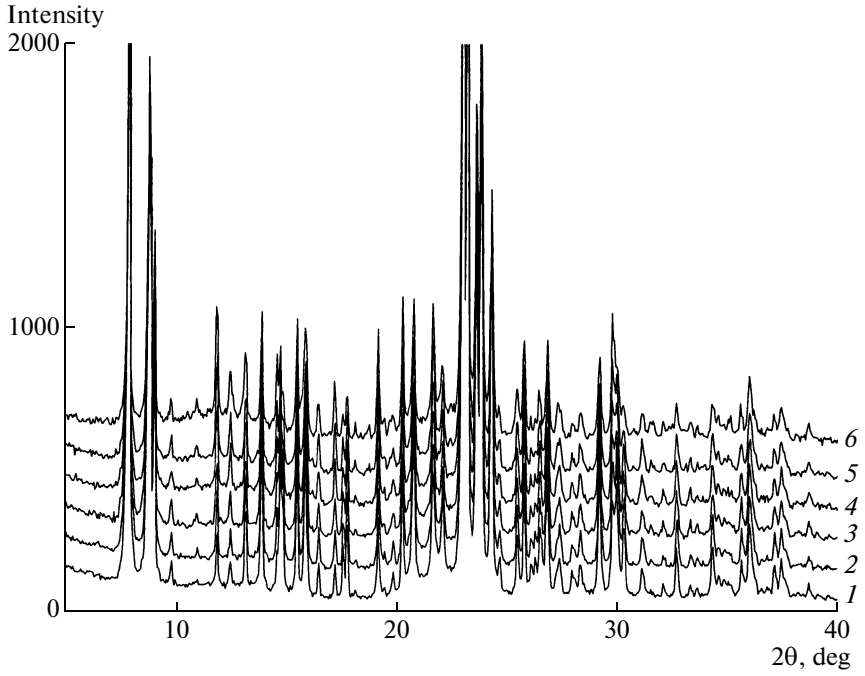

Fig. 9. X-ray diffraction patterns of (*1*) the parent HZSM-5 zeolite and (*2–6*) Cu(*n*)ZSM-5 samples: n = (*2*) 0.5, (*3*) 1, (*4*) 2, (*5*) 3, and (*6*) >3 wt %.

$(-Ni^{2+}-O^{2-})_n$ most likely stabilized in the fine mesopores of HZSM-5 zeolite.

Thus, according to electronic diffuse reflectance spectrometric data, an insignificant portion of Ni^{2+}_{Oh} cations is stabilized at the ion-exchange positions of HZSM-5 zeolite channels. At Ni^{2+} cation concentrations of 1.0 wt % or higher, a portion of Ni^{2+} cations is stabilized as two-dimensional oxygen-containing nanoclusters in fine mesopores of the zeolite. As the concentration of Ni^{2+} cations is increased to 3.0 and 5.0 wt %, the modifier component is also stabilized as the NiO oxide on the external surface of zeolite crystallites.

Figures 9 and 10 show the X-ray diffraction patterns of parent zeolite samples and zeolites with various concentrations of Cu (Fig. 9) and Ni (Fig. 10). From these data, it follows that the modified samples did not exhibit a noticeable shift of peaks with respect to the parent zeolite (for both Cu and Ni). However, depending on metal concentrations, a redistribution of line intensities was detectable (as compared with lines whose intensity remained constant): for example, the intensities of lines corresponding to the interplanar distances d/n = 11.19, 10.03, 6.37, 6.01, and 3.65 Å (2θ = 7.91°, 8.82°, 13.90°, 14.75°, and 24.36°) decreased with increasing concentrations of both copper and nickel, whereas the intensities of lines with d/n = 7.45, 7.09, 6.07, and 5.14 Å (2θ = 11.89°, 12.49°, 14.60°, and 17.24°) increased. The nickel-containing samples also exhibited a peak with d/n = 2.09 Å in the X-ray diffraction patterns; this peak corresponds to the strongest line of NiO, and its intensity increased with nickel content (this peak was absent from the parent zeolite). The sizes of coherent-scattering regions for NiO particles (in samples with concentrations of 3 and 5%) were ~80–100 nm. The most intense line of the $NiAl_2O_4$ phase (2θ = 37.04°) overlapped with zeolite lines; therefore, the presence of this phase cannot be reliably detected. In the copper-containing samples, it is difficult to detect phases (CuO and $CuAl_2O_4$) because the most intense lines of these phases (2θ = 35.53° and 36.90°, respectively) overlap with the lines of the parent zeolite.

As a result of the above studies, we can make the following conclusions: In the Cu(*n*)ZSM-5 and Ni(*n*)ZSM-5 catalysts, the modifier component contained copper and nickel only in a doubly charged state primarily in an octahedral oxygen environment. This allowed us to identify the stoichiometry of M^{2+}–oxygen fragments in the modifier component as MO and to compare its apparent density with the densities of bulk CuO and NiO oxides. We were the first to determine that the apparent densities of copper- and nickel-containing components arranged in the pore space of the zeolite are lower than the densities of bulk CuO and NiO phases by factors of ~3 and 4, respectively, because of a size effect.

The main regularities of the distribution of a modifier component in the Cu(*n*)ZSM-5 and Ni(*n*)ZSM-5 catalysts were dramatically different from one another. In both systems, a comparatively small fraction of doubly charged cations was stabilized at ion-

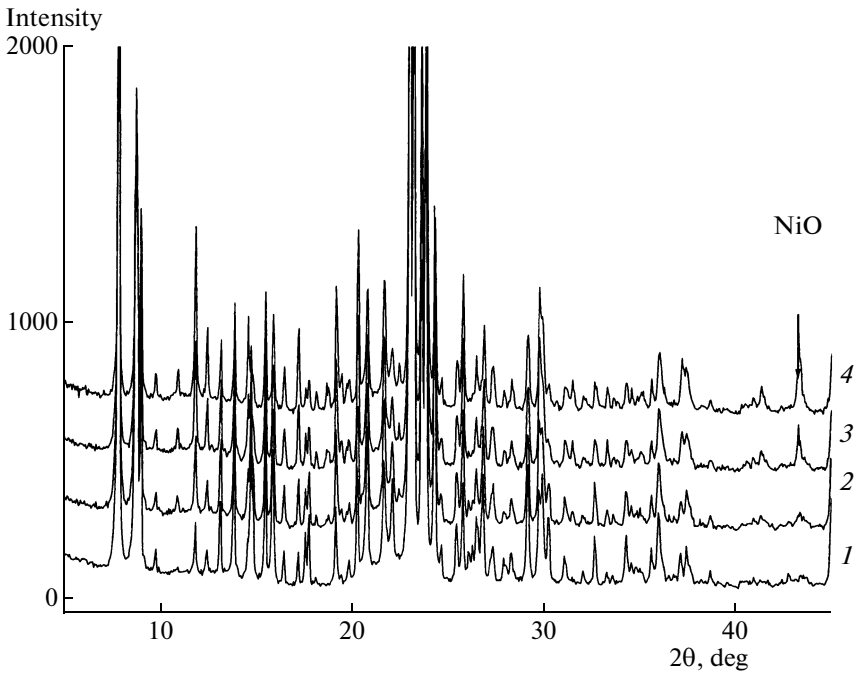

Fig. 10. X-ray diffraction patterns of (*1*) the parent HZSM-5 zeolite and (*2–4*) Ni(*n*)ZSM-5 samples: n = (*2*) 1, (*3*) 3, and (*4*) 5 wt %.

exchange positions as isolated M^{2+}_{Oh} ions. As the concentration of M^{2+} in the catalysts was increased, the fraction of ion-exchange M^{2+}_{Oh} somewhat increased. For Cu(*n*)ZSM-5 catalyst samples at $n > 1\%$, the degree of micropore filling with the modifier was approximately constant and amounted to ~10 vol %. The predominant filling of the finest mesopores with $D < 3.2$ nm was unexpected, whereas a portion of larger mesopores remained almost unfilled. Thus, in the Cu(*n*)ZSM-5 samples, the modifier was localized in zeolite channels (micropores) as Cu^{2+}_{Oh} mainly at ion-exchange positions, and, probably, in the structure of one-dimensional CuO nanoclusters and as two-dimensional oxide clusters in fine mesopores. We did not detect three-dimensional nanoparticles or coarsely dispersed particles of CuO in the pore space of the support.

For Ni(*n*)ZSM-5 catalysts, an approximately uniform distribution of the modifier in the pore space of mesopores and the absence of the modifier in zeolite channels (micropores) were found. The above effect of the partial blocking of channel throats with the modifier arranged on the surface of zeolite crystallites can be a reason for this phenomenon. At the same time, we detected a small amount of sufficiently large NiO crystals with a coherent-scattering region of 80–100 nm arranged on the external surface of zeolite powder particles. The considerable difference in the characters of modifier distributions in the Cu(*n*)ZSM-5 and Ni(*n*)ZSM-5 catalysts requires a discussion of possible reasons for the effects found.

The polycondensation processes of aqua Cu^{2+} and Ni^{2+} cations in the pore space of HZSM-5 zeolites were almost not studied, whereas these processes were studied in sufficient detail in aqueous solutions. Not only the hydrolysis of aqua cations but also the formation of polynuclear M^{2+} hydroxo complexes occurred on the preparation and alkalization of Cu^{2+} and Ni^{2+} salt solutions. For aqua Cu^{2+} cations, the formation of $CuOH^+$, Cu_2OH^{3+}, $Cu_2(OH)^{2+}_2$, $Cu_3(OH)^{4+}_2$, and $Cu_3(OH)^{2+}_4$ has been demonstrated [26, 27, 36]. Henceforth, all of the cations in the hydroxo complexes occur in an octahedral oxygen environment. In the general case, the set of $NiOH^+$, Ni_2OH^{3+}, $Ni_3(OH)^{3+}_3$, and $Ni_4(OH)^{4+}_4$ complexes is formed upon the polycondensation of aqua Ni^{2+} cations under comparable conditions [37]. It is believed that the last two complexes exhibit a closed cyclic structure. As the concentration of M^{2+} and the pH values of solutions were increased, the fraction of polynuclear hydroxo complexes increased and became predominant. A principal difference of $[Cu_3]$ complexes from $[Ni_3]$ and $[Ni_4]$ is that the $Cu_3(OH)^{4+}_2$ complexes in aqueous solutions exhibit only a linear structure due to the Jahn–Teller effect of copper [38]. Therefore, it is believed that, on the treatment of zeolite impregnated with salt solutions with an alkali in the case of a nickel-containing modifier, bulky complexes are formed in mesopores, and these complexes cannot penetrate into zeolite channels (micropores), whereas the linear

$Cu_3(OH)_2^{4+}$ complexes can, in principle, partially occupy these channels. The arrangement of the copper-containing modifier in the finest mesopores can be due to the formation of stronger bonds of the linear complexes with the pore surface of these sizes (Fig. 2). In general, the experimental results obtained in this work and the hypotheses proposed allowed us to explain differences in the characters of distribution of the modifier components in the Cu(*n*)ZSM-5 and Ni(*n*)ZSM-5 catalysts.

ACKNOWLEDGMENTS

This work was supported in part by the Russian Foundation for Basic Research (project no. 06-03-33107).

REFERENCES

1. Kharas, K.C.C., Liu Di-Jia, and Robota, H.J., *Catal. Today*, 1995, vol. 26, no. 2, p. 129.
2. Moretti, G., Dossi, C., Fusi, A., Recchia, S., and Psaro, R., *Appl. Catal., B*, 1999, vol. 20, no. 1, p. 67.
3. Iwamoto, M., Yahiro, H., Torikai, Y., Yoshioka, T., and Mizuno, N., *Chem. Lett.*, 1990, no. 11, p. 1967.
4. Lisi, L., Pirone, R., Ruoppolo, G., and Russo, G., *Kinet. Katal.*, 2008, vol. 49, no. 3, p. 442 [*Kinet. Catal.* (Engl. Transl.), vol. 49, no. 3, p. 421].
5. Moretti, G., Ferraris, G., Fierro, G., Jacono, M.L., Morpurgo, S., and Faticanti, M., *J. Catal.*, 2005, vol. 232, no. 2, p. 476.
6. Groothaert, M.H., Lievens, K., Leeman, H., Weckhuysen, B.M., and Schoonheydt, R.A., *J. Catal.*, 2003, vol. 220, no. 2, p. 500.
7. Kucherov, A.V., Kucherova, T.N., Nissenbaum, V.D., and Slinkin, A.A., *Kinet. Katal.*, 1995, vol. 36, no. 5, p. 731.
8. Sato, S., Yu-U, Y., Yahiro, H., Mizuno,N., and Iwamoto, M., *Appl. Catal., A*, 1990, vol. 70.
9. Burch, R. and Millington, P.J., *Appl. Catal., B*, 1993, vol. 2, no. 1, p. 101.
10. D'Itni, J.L. and Sachtler, W.M.H., *Catal. Lett.*, 1992, vol. 15, no. 1, p. 289.
11. Petunchi, J.O., Sill, G., and Hall, W.K., *Appl. Catal., B*, 1993, vol. 2, no. 4, p. 303.
12. Arishtirova, K., Dimitrov, Chr., Dyrek, K., Hallmeier, K.-Hz., Popova, Z., and Witkowski, S., *Appl. Catal., A*, 1992, vol. 81, no. 1, p. 15.
13. Kumar, N., Byggningsbacka, R., and Lindfors, L.-E., *React. Kinet. Catal. Lett.,* 1997, vol. 61, no. 2, p. 297.
14. Huang, X., Sun, X., Zhu, S., and Liu, Z., *React. Kinet. Catal. Lett.*, 2007, vol. 91, no. 2, p. 385.
15. Kubacka, A., Wang, Z., Sulikowski, B., and Corberan, V.C., *J. Catal.*, 2007, vol. 250, no. 1, p. 184.
16. Li, Y. and Armor, J.N., *Appl. Catal., B,* 1992, vol. 1, no. 4, p. L31.
17. Tang, Y., Zhang, T., Ma, L., Li, L., Zhao, Y., Zheng, M., and Lin, L., *Catal. Lett.*, 2001, vol. 73, no. 1, p. 193.
18. Li, W-Y., Jie, F., and Xie, K.-C., *Pet. Sci. Technol.*, 1998, vol. 16, nos. 5–6, p. 539.
19. Halliche, D., Cherifi, O., and Auroux, A., *Termochim. Acta*, 2005, vol. 434, no. 1, p. 125.
20. Inui, T., Makino, Y., Okazumi, F., Nagano, S., and Miyamoto, A., *Ind. Eng. Chem. Res.*, 1987, vol. 26, no. 3, p. 647.
21. Ihm, S.K., Yi, K.H., and Park, Y.K., *Stud. Surf. Sci. Catal.*, 1994, vol. 84, p. 1765.
22. Hoang, D.L., Berndt, H., Miessner, H., Schreier, E., Volter, J., and Lieske, H., *Appl. Catal., A*, 1994, vol. 114, no. 2, p. 295.
23. Kazansky, V.B., *J. Catal.*, 2003, vol. 216, nos. 1–2, p. 192.
24. Rice, M.J., Chakraborty, A.K., and Bell, A.T., *J. Catal.*, 2000, vol. 194, no. 2, p. 278.
25. Dedecek, J., Kaucky, D., Wichterlova, B., and Gonsiorova, O., *Phys. Chem. Chem. Phys.,* 2002, vol. 4, no. 21, p. 5406.
26. Perrin, D.D., *J. Chem. Soc.*, 1960, p. 3189.
27. Ohtaki, H., *Inorg. Chem.*, 1968, vol. 7, no. 6, p. 1205.
28. Krivoruchko, O.P., Anufrienko, V.F., Paukshtis, E.A., Larina, T.V., Burgina, E.B., Yashnik, S.A., Ismagilov, Z.R., and Parmon, V.N., *Dokl. Akad. Nauk*, 2004, vol. 398, no. 3, p. 356 [*Dokl. Phys. Chem.* (Engl. Transl.), vol. 398, Part 1, p. 226].
29. Krivoruchko, O.P., Gavrilov, V.Yu., Molina, I.Yu., and Larina, T.V., *Kinet. Katal.*, 2008, vol. 49, no. 2, p. 300 [*Kinet. Catal.* (Engl. Transl.), vol. 49, no. 2, p. 285].
30. Karnaukhov, A.P., *Adsorbtsiya: Tekstura dispersnykh i poristykh materialov* (Adsorption: Texture of Disperse and Prous Materials), Novosibirsk: Nauka, 1999.
31. Gregg, S.J. and Sing, K.S.W., *Adsorption, Surface Area and Porosity*, London: Academic, 1982.
32. Mott, N. and Davis, E., *Electronic Processes in Non-Crystalline Materials*, Oxford: Oxford Univ., 1979.
33. Shinkarenko, V.G., *Cand. Sci. (Chem.) Dissertation*, Novosibirsk: Inst. of Catalysis, 1978.
34. Lever, A.B.P., *Inorganic Electronic Spectroscopy*, Amsterdam: Elsevier:, 1987.
35. Becerra, A.M. and Castro-Luna, A.E., *J. Chil. Chem. Soc*, 2005, vol. 50, no. 2, p. 465.
36. Karge, H.G., Wichterlova, B., and Beyer, H.K., *J. Chem. Soc., Faraday Trans.*, 1992, vol. 88, no. 9, p. 1345.
37. *Problemy sovremennoi khimii koordinatsionnykh soedinenii* (Current Topics in Coordination Chemistry), Shchukin, S.A. and Vasil'kov, I.V., Eds., Leningrad: Leningr. Gos. Univ., 1968, p. 134.
38. Kugel', K.I. and Khomskii, D.I., *Usp. Fiz. Nauk*, 1982, vol. 136, no. 4, p. 621.